

1 **Pneumolysin binds to the Mannose-Receptor C type 1 (MRC-1) leading to anti-**  
2 **inflammatory responses and enhanced pneumococcal survival**

3 Karthik Subramanian<sup>1#</sup>, Daniel R Neill <sup>2#</sup>, Hesham Malak<sup>2§</sup>, Laura Spelmink<sup>1§</sup>, Shadia  
4 Khandaker<sup>2</sup>, Giorgia Dalla Libera Marchiori<sup>1</sup>, Emma Dearing<sup>2</sup>, Alun Kirby<sup>3</sup>, Marie Yang<sup>2</sup>,  
5 Adnane Achour<sup>4</sup>, Johan Nilvebrant<sup>5</sup>, Per-Åke Nygren<sup>5</sup>, Laura Plant<sup>1</sup>, Aras Kadioglu<sup>2\*#</sup>,  
6 Birgitta Henriques-Normark<sup>1,6,7\*#</sup>

7  
8 <sup>1</sup> Department of Microbiology, Tumor and Cell Biology, Karolinska Institutet, SE-171 77  
9 Stockholm, Sweden.

10 <sup>2</sup> Institute of Infection and Global Health, Ronald Ross Building, 8 West Derby Street,  
11 University of Liverpool, Liverpool, UK.

12 <sup>3</sup> Centre for Immunology and Infection, Department of Biology and Hull York Medical School,  
13 University of York, York, UK.

14 <sup>4</sup> Science for Life Laboratory, Department of Medicine Solna, Karolinska Institutet, and  
15 Department of Infectious Diseases, Karolinska University Hospital, Solna, Stockholm, SE,  
16 17176, Sweden.

17 <sup>5</sup> Division of Protein Technology, School of Biotechnology, Royal Institute of Technology  
18 (KTH), SE-106 91 Stockholm, Sweden.

19 <sup>6</sup> Clinical Microbiology, Karolinska University Hospital, SE-171 76 Stockholm, Sweden.

20 <sup>7</sup> Lee Kong Chian School of Medicine (LKC) and Singapore Centre on Environmental Life  
21 Sciences Engineering (SCELSE), Nanyang Technological University, Singapore 639798,  
22 Singapore.

23  
24 # Co-first authors

25 # Co-senior authors

26 § These authors contributed equally

27 \*Correspondence to Prof. Birgitta Henriques-Normark (birgitta.henriques@ki.se) and Prof.  
28 Aras Kadioglu (a.kadioglu@liverpool.ac.uk)

29

30 **Abstract**

31 *Streptococcus pneumoniae* (the pneumococcus) is a major cause of mortality and morbidity  
32 globally, and the leading cause of death in under-five year olds. The pneumococcal cytolysin  
33 pneumolysin (PLY) is a major virulence determinant, known to induce pore-dependent pro-  
34 inflammatory responses. These inflammatory responses are driven by PLY-host cell membrane  
35 cholesterol interactions, with binding to a host cell receptor not previously demonstrated.  
36 However, here we discovered a receptor for PLY, whereby pro-inflammatory cytokine  
37 responses and TLR signaling are inhibited upon PLY binding to the Mannose-Receptor C type  
38 1 (MRC-1) in human dendritic cells (DCs) and murine alveolar macrophages, along with  
39 upregulation of the cytokine suppressor SOCS1. Moreover, PLY-MRC-1 interaction mediates  
40 pneumococcal internalization into non-lysosomal compartments and polarizes naive T cells into  
41 an IFN- $\gamma^{\text{low}}$ , IL-4 $^{\text{high}}$  and FoxP3 $^+$  immunoregulatory phenotype. In mice, PLY-expressing  
42 pneumococci co-localize with MRC-1 in alveolar macrophages, and induce lower pro-  
43 inflammatory cytokine responses and reduced neutrophil infiltration, compared to a PLY-  
44 mutant. *In vivo*, MRC-1-inhibition using blocking antibodies or MRC-1 deficient mice, show  
45 reduced bacterial loads in the airways. In conclusion, we show that pneumococci use PLY-  
46 MRC-1 interactions to downregulate inflammation and enhance bacterial survival in the  
47 airways. This has important implications for future vaccine design.

48

49

50

51 **Main Text**

52 *Streptococcus pneumoniae* is a common colonizer of the upper respiratory tract of healthy  
53 children, but also a major cause of life-threatening diseases such as pneumonia, septicaemia  
54 and meningitis, resulting in death of over 800,000 children annually<sup>1</sup>. The cholesterol-binding  
55 pore-forming toxin pneumolysin (PLY) is expressed by most disease-causing isolates and is  
56 required for virulence<sup>2,3</sup> and host-to-host transmission<sup>4</sup>. PLY is a multi-functional protein,  
57 which at sublytic doses can activate complement<sup>5</sup>, re-arrange cytoskeleton of host cells<sup>6</sup>, and  
58 induce pro-inflammatory cytokine responses<sup>7</sup>. PLY is released during bacterial autolysis, but  
59 has also been shown to be localized on the pneumococcal cell wall, thereby accessible to  
60 extracellular proteases<sup>8</sup>. The surface localization of PLY allows for speculation of a non-  
61 cholesterol receptor on host cells.

62 Alveolar macrophages and dendritic cells (DCs) are the major resident immune cells in alveoli  
63 and mediate protection from pathogens. The mannose receptor, MRC-1 (CD206), is a M2  
64 phenotype marker<sup>9</sup> and a phagocytic receptor<sup>10</sup> that is mostly expressed by tissue macrophages,  
65 including alveolar macrophages<sup>11</sup>. MRC-1 binds to endogenous and microbial antigens such as  
66 capsular polysaccharides<sup>12,13</sup>. Furthermore, studies have demonstrated that MRC-1 influences  
67 pneumococcal uptake by Schwann and olfactory cells, but they did not show co-  
68 localization<sup>14,15</sup>. It is not clear which macrophage receptors recognize pneumococci in the  
69 nasopharynx and lungs and what bacterial properties interacts with the receptors mediating  
70 pneumococcal uptake. Here, we discovered a role for PLY in driving anti-inflammatory  
71 responses and lysosomal escape in macrophages and DCs by directly binding to MRC-1,  
72 thereby promoting pneumococcal internalization and survival in the host.

73 We first compared the cytokine response induced by PLY by infecting different immune cells,  
74 primary human monocyte-derived dendritic cells (DCs), neutrophils and THP-1 monocyte-  
75 derived macrophages, with a low dose (MOI of 1) of the pneumococcal strain T4R (expressing

76 PLY), or its isogenic PLY mutant T4R $\Delta$ ply. The non-encapsulated strain T4R (isogenic  
77 capsular mutant of the encapsulated serotype 4 strain T4) was used for the *in vitro* experiments  
78 to increase bacterial uptake since the capsule impedes bacterial adhesion to host cells<sup>16</sup>. We  
79 found lower secretion of the pro-inflammatory cytokines TNF- $\alpha$ , IL-1 $\beta$  and IL-12 from DCs  
80 challenged with PLY-proficient T4R compared to the mutant T4R $\Delta$ ply, which was in contrast  
81 to THP-1-derived macrophages and neutrophils (Fig.1a, Supplementary Fig.1a-b). This PLY-  
82 dependent inhibition of cytokine responses was also observed using the encapsulated strains T4  
83 and T4 $\Delta$ ply (Fig.1b). The cytokine inhibition was independent of cell death as determined by  
84 measuring LDH release (Supplementary Fig.1c), but dependent on bacterial uptake since  
85 secretion of TNF- $\alpha$  was reduced by blocking phagocytosis using cytochalasin D and  
86 wortmannin (Supplementary Fig.1d). Treatment with cytochalasin D, an inhibitor of actin  
87 polymerization, inhibited cytokine production by DCs and THP-1 macrophages in a PLY-  
88 independent manner. Pre-treatment with purified endotoxin-free PLY at 100 ng/ml inhibited  
89 IL-12 production by ~50% from DCs infected with T4R $\Delta$ ply in a dose-dependent manner,  
90 independent of cell death (Supplementary Fig.1e). To study strain dependency and the influence  
91 of the challenge dose we then infected DCs, THP-1 macrophages, neutrophils and bone-marrow  
92 derived macrophages (BMDMs) with the pneumococcal strains D39 of serotype 2, or its  
93 isogenic PLY mutant, D39 $\Delta$ ply, at different MOIs and measured IL-1 $\beta$  release and cell death  
94 (Supplementary Fig.1f-i). We observed that at lower infection doses (MOI of 0.1 or 1), the  
95 mutant D39 $\Delta$ ply induced higher levels of IL-1 $\beta$  in DCs and BMDMs (but not in neutrophils  
96 and THP-1 macrophages), independent of cell death. However, at MOI of 10, the pattern was  
97 reversed and wild-type D39 induced higher IL-1 $\beta$  release, but this was also accompanied by ~2  
98 fold higher cell death.

99 We then performed a TLR signalling q-PCR array using RNA from DCs infected for 9hrs with  
100 T4R or T4R $\Delta$ ply. Expression of all genes, except IFN $\beta$ 1, was upregulated following infection

101 with T4R $\Delta$ ply compared to T4R infected cells (Supplementary Fig.1j), indicating that PLY-  
102 expression has a general inhibitory effect on cytokine induction and inflammatory signalling in  
103 DCs.

104 To explore mechanisms behind this inhibitory effect of PLY on DCs, we measured expression  
105 of the negative regulators of NF- $\kappa$ B, AP-1 and STAT1 pro-inflammatory signalling pathways.  
106 We identified upregulation of Suppressor of Cytokine Signalling 1, SOCS1<sup>17</sup>, mRNA in DCs  
107 infected with T4R, but not with T4R $\Delta$ ply (Fig.1c). Kinetic analysis revealed that SOCS1 mRNA  
108 increased 6hrs post infection (pi) and peaked at 9hrs (Supplementary Fig.1k). Concurrent with  
109 mRNA, protein levels of SOCS1 were higher in DCs at 9hrs pi with T4R compared to T4R $\Delta$ ply  
110 (Fig.1d). However, SOCS1 expression remained unaffected in THP-1 macrophages,  
111 (Supplementary Fig.1l), confirming the cell-type specific effect.

112 Since SOCS1 is a known inhibitor of STAT signalling<sup>18</sup>, we measured phosphorylated STAT1  
113 and found delayed phosphorylation in T4R-infected DCs as compared to T4R $\Delta$ ply (Fig.1e).  
114 Pre-treatment with the STAT inhibitor stattic inhibited secretion of TNF- $\alpha$ , IL-1 $\beta$  and IL-12  
115 (Supplementary Fig.1m-o). Besides STAT1, we also found lower levels of NF- $\kappa$ B in T4R-  
116 infected DCs compared to T4R $\Delta$ ply (Fig.1f). Together, our data suggest that PLY-expression  
117 inhibits pro-inflammatory signalling via STAT1 and NF- $\kappa$ B in DCs, possibly via induction of  
118 the cytokine suppressor, SOCS1.

119 To identify the host receptor interacting with PLY, we performed a pull-down assay using  
120 purified PLY. We identified 32 proteins exclusively from DC lysates of which three were  
121 surface proteins, Integrin alpha-M, Mannose Receptor C type 1 (MRC-1), and Galectin-1  
122 (Supplementary Table 1). We further investigated the lectin receptor MRC-1, since it has  
123 previously been reported to have immunosuppressive properties<sup>19</sup>. To confirm the interaction  
124 between MRC-1 and PLY, we performed immunoprecipitation of MRC-1 from native DC

125 lysates using anti-PLY coupled beads (Supplementary Fig.2a). To assess whether MRC-1  
126 binding to PLY was mediated via glycan recognition, we performed enzymatic deglycosylation  
127 of PLY to remove bound glycans as evident by slightly higher electrophoretic gel mobility  
128 (Supplementary Fig.2b). Importantly, MRC-1 co-immunoprecipitated with both native and  
129 deglycosylated PLY from native DC lysates (Supplementary Fig.2c). We found that MRC-1  
130 was selectively expressed by DCs and M-CSF derived macrophages (M2 polarized), but not by  
131 THP-1, neutrophils or GM-CSF derived macrophages (M1 polarized) (Supplementary Fig.2d-  
132 e). Interestingly, DCs upregulated MRC-1 expression upon infection with T4R, compared to  
133 T4R $\Delta$ ply (Supplementary Fig.2f). Similar to human DCs, BMDMs isolated from wild-type, but  
134 not MRC-1<sup>-/-</sup> mice, upregulated the MRC-1 protein upon infection with strain D39 as compared  
135 to its isogenic PLY-deficient mutant, D39 $\Delta$ ply (Supplementary Fig.2g). The capsular mutant  
136 (D39 $\Delta$ cps) induced lower upregulation of MRC-1 than D39 (Supplementary Fig.2h). Analysis  
137 of MRC-1 expression at different MOIs revealed that DCs and BMDMs upregulated MRC-1 in  
138 a dose-dependent way in response to D39, as compared to D39 $\Delta$ ply, and the difference was  
139 significant at MOI of 1 (Supplementary Fig.2i-l). Neutrophils and THP-1 macrophages showed  
140 very low MRC-1 expression that did not change significantly upon infection. Surface plasmon  
141 resonance analysis confirmed the PLY-MRC-1 interaction showing a  $K_D$  value of  $4.5 \times 10^{-8}$  M  
142 (Fig.2a). The interaction was also verified in the reverse orientation (Supplementary Fig.2m),  
143 and the specificity was shown using control proteins (Supplementary Fig.2n). To study the  
144 specific interaction of MRC-1 with PLY versus capsular polysaccharides, we performed ELISA  
145 to measure binding of immobilized MRC-1 with PLY dose-dependently in the presence or  
146 absence of purified serotype 2 or 4 capsules. We found that MRC-1 binds to the type 2, but not  
147 the type 4 capsule (Supplementary Fig.2o). Importantly, MRC1 still binds to PLY even in the  
148 presence of capsule although to lesser extent (Supplementary Fig.2o). To identify the region of  
149 interaction, we performed a solid-phase binding assay using purified PLY domains and an Fc-

150 construct containing the mannose-binding C-type lectin-like carbohydrate recognition domains  
151 of MRC-1 (CTLD4-7-Fc). We found that domain 4 of PLY is key to MRC-1-PLY-interaction  
152 as purified domain 4, but not domains 1-3, bound the CTLD4-7-Fc construct (Fig. 2b). The  
153 non-pore-forming PLY mutant (PdB)<sup>20</sup> showed reduced binding compared to cytolytic PLY  
154 (Fig.2b), indicating that active PLY is required for MRC-1 binding.

155 Next, we investigated the localization patterns of MRC-1 and PLY in DCs using  
156 immunofluorescence microscopy. Wild-type DCs or MRC-1-deficient DCs (treated with MRC-  
157 1 siRNA), were incubated for 45 min with recombinant active PLY. PLY co-localized with  
158 MRC-1 and the early endosomal antigen EEA-1, indicating uptake by DCs (Fig.2c). In contrast,  
159 PLY-binding was reduced in MRC-1-deficient DCs. In addition, the non-pore- forming PLY  
160 mutant (PdB) did not co-localize with MRC-1 (Fig.2c). At 90 min post pneumococcal  
161 challenge, internalized T4R co-localized with MRC-1, but did not co-localize with lysosomes,  
162 while the converse was observed for T4R $\Delta$ ply (Fig.2d). To test whether bacterial internalization  
163 via MRC-1 inhibits fusion of pneumococcal-infected vacuoles with lysosomes, we used  
164 antibody-opsonized pneumococci as a control to engage Fc gamma receptor-mediated  
165 phagocytosis<sup>21</sup>. Strikingly, opsonized T4 did not co-localize with MRC-1 and co-stained with  
166 lysosomes in contrast to the non-opsonized control (Supplementary Fig.2p). Moreover,  
167 opsonized T4 elicited similar levels of TNF- $\alpha$  and IL-1 $\beta$  from DCs as T4 $\Delta$ ply (Supplementary  
168 Fig.2q). To explore whether active PLY is required for interaction with MRC-1 in clinical  
169 pneumococcal isolates, we used a serotype 1 strain expressing non-haemolytic PLY (BHN31  
170 of ST306) and the clonally related haemolytic strain (BHN32 of ST228)<sup>22</sup>. We found that the  
171 non-haemolytic strain did not co-localize with MRC-1, but co-stained for lysosomes  
172 (Supplementary Fig.2r), and elicited higher cytokine production from DCs (Supplementary  
173 Fig.2s) as compared to the haemolytic strain. Together, our data suggest that pneumococcal  
174 internalization, due to interaction between active PLY and MRC-1, inhibits fusion of vacuoles

175 containing pneumococci with lysosomes. This is supported by previous findings that MRC-1  
176 regulates phagosomal trafficking following phagocytosis and limits fusion with lysosomes<sup>10,23</sup>.  
177 Furthermore, we found that uptake of PLY-proficient T4R, but not T4R $\Delta$ *ply*, was reduced by  
178 50% in MRC-1 depleted DCs (Fig.3a and Supplementary Fig.3a). Also, depletion of MRC-1 in  
179 DCs led to significantly higher levels of IL-12, TNF- $\alpha$  and IL-6 upon T4R-infection (Fig.3b),  
180 and abrogated SOCS1 expression (Supplementary Fig.3b). This suggests that activation of  
181 MRC-1 by PLY triggers upregulation of SOCS1 in DCs, thereby reducing secretion of  
182 inflammatory cytokines.

183 Since DCs are professional antigen-presenting cells, we investigated the role of MRC-1 in DC-  
184 primed CD4<sup>+</sup> T-helper cell cytokine responses after pneumococcal challenge. We found that  
185 DCs depleted of MRC-1 using siRNA and infected with T4R (in contrast to T4R $\Delta$ *ply*), elicited  
186 higher IFN- $\gamma$  (Th1 cytokine) and lower IL-4 (Th2 cytokine) levels from naive T-helper cells in  
187 co-culture, compared to DCs treated with control siRNA (Fig.3c-d). A similar trend was  
188 observed in DCs stimulated with purified PLY. To further characterize the phenotype of T cells  
189 co-cultured with DCs, we measured FoxP3, a regulatory T cell marker<sup>24</sup> and found that DCs  
190 infected with T4R (but not with T4R $\Delta$ *ply*) and those treated with purified PLY, induced higher  
191 FoxP3 expression in naive T helper cells upon co-culture (Fig.3e, Supplementary Fig.3c).  
192 FoxP3 upregulation in T cells was abolished when co-cultured with DCs treated with MRC-1  
193 siRNA. Similar to human DCs, murine BMDMs from WT mice that were infected with D39  
194 (in contrast to D39 $\Delta$ *ply*) and co-cultured with CD4<sup>+</sup> murine T cells, resulted in higher regulatory  
195 (FoxP3, IL-10 expressing) T cells and lower Th1 cells (T-bet, IFN- $\gamma$  expressing) as compared  
196 to BMDMs from MRC-1<sup>-/-</sup> mice (Fig.3f, Supplementary Figs. 3d-f). Our data are in agreement  
197 with earlier findings showing that MRC-1 expression in DCs inhibits CD45 and induces T-cell  
198 tolerance<sup>25</sup>, and that PLY is required for robust regulatory T cell induction *in vivo*<sup>26</sup>.

199 To verify our findings *in vivo*, we challenged wild-type C57BL/6J mice intranasally with 10<sup>6</sup>  
200 CFU of wild-type T4 or the mutant T4 $\Delta$ *ply*. At 6hrs post infection (pi), bronchoalveolar lavage  
201 fluids (BALF) were collected and lung alveolar macrophages isolated. We observed  
202 intracellular co-localization of strain T4 with MRC-1, but not with lysosomes (Fig.4a). In  
203 contrast, intracellular T4 $\Delta$ *ply* did not co-localize with MRC-1, but co-stained with lysosomes  
204 (Fig.4a, Supplementary Fig.4a). *Ex vivo*, murine alveolar macrophages secreted lower levels of  
205 pro-inflammatory cytokines upon infection with T4R compared to T4R $\Delta$ *ply*. This difference  
206 was reduced by pre-treatment with anti-MRC-1 (Supplementary Fig.4b-c). In agreement with  
207 these results, T4 $\Delta$ *ply* infected mice had higher levels of pro-inflammatory cytokines, TNF- $\alpha$ ,  
208 IL-12 and IL-1 $\beta$ , and lower levels of anti-inflammatory cytokines, IL-10 and TGF- $\beta$ , in the  
209 BALF, compared to mice infected with T4 (Fig.4b, Supplementary Fig. 4d). In addition, T4 $\Delta$ *ply*  
210 infected mice had higher numbers of neutrophils and monocytes in the BALF (Supplementary  
211 Fig.4e). The enhanced inflammation and higher infiltration of phagocytes were concurrent with  
212 the higher clearance of T4 $\Delta$ *ply* compared to T4 from the airways of infected mice (Fig.4c).  
213 Mice pre-treated with antibodies to block MRC-1 prior to infection with T4 had significantly  
214 higher levels of TNF- $\alpha$  and IL-12, and lower levels of IL-10 in BALF at 6hrs pi as compared  
215 to isotype antibody-treated controls (Fig.4d, Supplementary Fig.4f). Anti-MRC-1 treated mice  
216 had 50% lower bacterial counts in the lower airways compared to controls (Fig.4e), and  
217 intracellular bacteria did not co-localize with MRC-1 in alveolar macrophages (Supplementary  
218 Fig.4g). Importantly, MRC-1<sup>-/-</sup> mice also had significantly decreased bacterial numbers in the  
219 nasopharynx at 7 and 14 days post challenge compared to wild-type mice in a pneumococcal  
220 carriage model with strain D39 (Fig.4f). In wild-type mice, MRC-1<sup>+</sup> macrophages were found  
221 to rapidly accumulate in the nasopharynx following pneumococcal colonization  
222 (Supplementary Fig.5a-b). Similar to anti-MRC-1 treated mice, MRC-1<sup>-/-</sup> mice had higher  
223 levels of pro-inflammatory cytokines, TNF- $\alpha$  and IL-6, and lower levels of anti-inflammatory

224 IL-10 and TGF- $\beta$  in the nasopharynx compared to WT mice at 6hrs and 1 day pi (Supplementary  
225 Fig.5c-f).

226 MRC-1 mediated phagocytosis is of particular significance in the lungs, as MRC-1 is  
227 abundantly expressed by alveolar macrophages. A previous study by Dorrington et al.  
228 highlighted the crucial role of the scavenger receptor MARCO in anti-pneumococcal immunity  
229 in the nasopharynx and suggested a minimal role for MRC-1<sup>27</sup>. However, the authors in that  
230 study used a 100-fold higher infection dose ( $1 \times 10^7$  CFU) for colonization compared to our study  
231 and we have previously shown that in contrast to high-density infection, low density  
232 pneumococcal carriage induces immunoregulatory responses characterized by sustained  
233 elevation of nasopharyngeal TGF- $\beta$ 1, regulatory T cells and MRC-1 expressing macrophages<sup>26</sup>.  
234 In the current study, we demonstrate that the infection dose determines the nature of cytokine  
235 response to PLY, where lower infection doses eliciting cytokine inhibition. Hence, our results  
236 suggest that the infection dose is critical when studying host responses to pneumococcal  
237 infections.

238 PLY is not a typical adhesin and has previously been considered to be cytosolic and released  
239 only upon bacterial lysis. However, recent data using transmission electron microscopy<sup>28</sup> show  
240 that pneumolysin can be surface localized, suggesting that it can be available for interactions  
241 with host receptors. The above data support our discovery that PLY interacts with MRC-1  
242 which is a finding that represents a conceptual change in our current understanding. Our results  
243 suggest that MRC-1-PLY interaction is not mediated by glycan recognition, since MRC-1 also  
244 binds to deglycosylated PLY, and the interaction is specifically mediated by C type lectin  
245 domains 4-7 of MRC-1 and domain 4 of PLY.

246 In conclusion, we discovered a significant role for PLY, whereby MRC-1 acts as a receptor for  
247 PLY, enabling pneumococci to invade MRC-1 proficient immune cells including DCs and

248 alveolar macrophages in the airways, thereby dampening cytokine responses to establish  
249 intracellular residency of pneumococci. Whilst MRC-1 has previously been demonstrated to  
250 bind pneumococcal capsular polysaccharides<sup>12,13</sup>, we show here that it can also directly bind to  
251 PLY. This is a hitherto unknown survival mechanism for the pneumococcus and has important  
252 implications for future vaccine design against infection. The potential mechanisms involved are  
253 summarized in Fig.4g.

254

255

## 256 **Methods**

### 257 **Pneumococcal strains used**

258 The encapsulated *S. pneumoniae* serotype 4 strain TIGR4 (T4; ATCC BAA-334) as well as its  
259 non-encapsulated isogenic mutant, T4R, and their isogenic PLY-deficient mutants T4 $\Delta$ ply and  
260 T4R $\Delta$ ply were used in this study. Clinical isolates of serotype 1 pneumococci expressing non-  
261 hemolytic PLY (BHN31 of ST306) or clonally related strain expressing haemolytic PLY,  
262 (BHN32 of ST 228) were also used<sup>22</sup>. Bacteria were grown on blood agar plates at 37°C and  
263 5% CO<sub>2</sub> overnight. Colonies were inoculated into C+Y medium and grown until exponential  
264 phase (OD<sub>620</sub> = 0.5). For opsonisation, pneumococci were incubated with 5% Type 4 anti-serum  
265 for 30 min at 37°C (Statens Serum Institut).

266 *S. pneumoniae* serotype 2, strain D39 (NCTC 7466), was obtained from the National Collection  
267 of Type Culture, London, UK. The pneumolysin-deletion D39 mutant D39 $\Delta$ ply was kindly  
268 provided by Prof. Tim Mitchell (University of Birmingham). Capsular-deficient D39-J  
269 (D39 $\Delta$ cps) and the double mutant in PLY and the capsule DKO (double knock out)  
270 (D39 $\Delta$ cps $\Delta$ ply) were kindly provided by Dr. Lucy Hathaway (University of Bern). D39 was  
271 cultured on blood agar base with 5% v/v horse blood, or in brain heart infusion broth (BHI;  
272 Oxoid, Basingstoke, UK) with 20% v/v FBS (Sigma), Supplementaryemented with 20 mg/ml  
273 spectinomycin (Sigma) for DKO.

### 274 **Pneumolysin (PLY)**

275 Recombinant PLY, mutant (PdB) or PLY domains (D1-3, D4), were expressed in *E. coli* and  
276 purified as previously described<sup>7</sup>. PLY D1-3 and D4 were kindly provided by Prof. Tim  
277 Mitchell (University of Birmingham). Haemolytic activity of PLY was 100,000 HU/mg.  
278 Purified toxin was passed six times through an endotoxin removal column (Profos AG,  
279 Germany) and absence of detectable LPS was confirmed with PyroGene Recombinant Factor  
280 C assay (Lonza; detection limit 0.01 EU/ml).

281 **Cell isolation from buffy coats, cell-culture and infection**

282 Monocytes were purified from buffy coats of healthy donors (Karolinska University Hospital  
283 and Uppsala University Hospital) using the RosetteSep™ monocyte purification kit (Stem Cell  
284 Technologies) and Ficoll-Paque Plus (GE Healthcare) gradient centrifugation. For  
285 differentiation into DCs, monocytes were cultured in R10 (RPMI 1640, 2 mM L-glutamine,  
286 10% FBS) supplemented with GM-CSF (40 ng/ml) and IL-4 (40 ng/ml) from  
287 Peprotech for 6 days. DCs were verified by flow cytometry to be >90% CD1a<sup>+</sup> CD11c<sup>+</sup>. In co-  
288 culture experiments, at 24 hrs post infection, DCs were washed and incubated with naïve CD4<sup>+</sup>  
289 T cells in a 1:10 ratio (DC: T cells) at 37°C. Supernatants were collected 5 days later for  
290 cytokine measurements by ELISA. Cytokine values were subtracted from control wells  
291 containing DCs alone. For infection, DCs were incubated with pneumococci at a multiplicity  
292 of infection (MOI) of 1 and extracellular bacteria were killed with 200 µg/ml gentamicin after  
293 2 hrs of infection. Cytochalasin D (0.5 mM), wortmannin (0.1 mM) (Sigma) or stattic (5 µM)  
294 (Tocris Biosciences) were added to cells 15 min prior to pneumococcal infection. In some  
295 experiments, DCs were incubated with endotoxin-free PLY at 0.2 µg/ml diluted in R10  
296 medium.

297 Human monocytic leukemia THP-1 cells (ATCC TIB-202) were cultivated in R10. For  
298 differentiation into macrophages, THP-1 cells were treated for 48 hrs with 20 ng/ml of phorbol  
299 myristate acetate (PMA) (Sigma).

300 Neutrophils were isolated from whole blood upon lysis of RBCs and enriched using the  
301 EasySep human neutrophil enrichment kit (StemCell Technologies) according to the  
302 manufacturer's instructions. Purified neutrophils were verified to be ~99% CD66b<sup>+</sup>CD16<sup>+</sup>.

303 Human naïve T cells were purified from fresh PBMCs using the EasySep™ Human Naive  
304 CD4<sup>+</sup> T Cell Isolation Kit (Stem cell Technologies) and were verified by flow cytometry to be  
305 >95% CD3<sup>+</sup>CD4<sup>+</sup>. All cells used in this study were mycoplasma tested.

306 **Isolation of mouse bone-marrow derived macrophage (BMDM) and culture**

307 Bone-marrow cells were flushed from murine femurs and tibia. Macrophages were grown from  
308 bone marrow cells in Dulbecco's Modified Eagle's Medium (Sigma, UK) 10% v/v foetal calf  
309 serum (FCS; Sigma), 100 U/ml penicillin, 100 mg/ml streptomycin, and 100 mM L-glutamine  
310 (Sigma) Supplementaryemented with 20 ng/ml macrophage colony-stimulating factor (M-CSF;  
311 R&D systems). Cultures were maintained in a humidified atmosphere (5% CO<sub>2</sub>) at 37°C, and  
312 medium was replaced on days 3 and 6. On day 6, cells were plated for use in assays. 6.25x10<sup>5</sup>  
313 BMDM were cultured alone (untreated) or infected with D39, D39Δply, D39Δcps or DKO  
314 (D39ΔcpsΔply)(1 macrophage: 10 bacteria) or stimulated with purified PLY (4 μg/ml). After  
315 24 hrs incubation, supernatants were collected and used to assess cytokine production by ELISA  
316 or determine density of infection by Miles and Misra dilution.

317 **BMDM-T cell co-culture**

318 Naive CD25<sup>-</sup>CD4<sup>+</sup> T cells were purified from spleen of C57BL/6 or MRC-1<sup>-/-</sup> mice by negative  
319 selection (Miltenyi Biotec). Non-CD4<sup>+</sup> T cells and CD44<sup>+</sup> memory T cells were labelled with  
320 biotinylated antibodies, before addition of anti-biotin microbeads and magnetic separation.  
321 CD4<sup>+</sup> T-cell purity was >90%. Purified T-cells were added to 24 hrs pneumococcal stimulated  
322 BMDM at a ratio of 15:1 for 5 days. Culture supernatants were collected for ELISA and cells  
323 were stained for flow cytometry.

324 **Cell viability assays**

325 Cytotoxicity was determined in the culture supernatants by measuring the release of the enzyme  
326 lactate dehydrogenase (LDH) compared to a 100% lysis control using the Cytotoxicity kit  
327 (Roche) according to manufacturer's instructions.

328

329 **Real time quantitative PCR (qPCR)**

330 Total cellular RNA was extracted from cells using the RNeasy Kit (Qiagen). The concentration  
331 and purity of isolated RNA was determined spectrophotometrically with the Nanodrop ND  
332 1000. cDNA was synthesized from the isolated RNA using the High Capacity cDNA Reverse  
333 Transcription kit (Applied Biosystems). The qPCR was performed using the iTaq Universal  
334 SYBR Green Supermix (BioRad) according to manufacturer's instructions. The following  
335 primers were used: Hs\_SOCS1\_1\_SG, Hs\_MRC1\_1\_SG and Hs\_GAPDH\_1\_SG. Each primer  
336 pair was validated for specificity by performing melt curve analysis of the PCR product to  
337 ensure the absence of primer dimers and unspecific products. The mRNA expression level was  
338 normalized to the level of GAPDH and relative expression was determined with the  $\Delta\Delta CT$   
339 method. The TLR Signaling qPCR array (Qiagen) was performed according to the  
340 manufacturer's instructions and analysed with the GeneGlobe Data analysis Center (Qiagen).

341 **Mouse experiments and isolation of alveolar macrophages**

342 All mice experiments were performed in accordance with the local ethical committee  
343 (Stockholms Norra djurförsöksetiska nämnd). Six- to seven- weeks old male wild-type  
344 C57BL/6J were used. Sample size was chosen to generate statistically significant data and based  
345 on pilot experiments to calculate variation within and between the experimental groups and  
346 probable degrees of freedom necessary to validate conclusions. Experiments with MRC-1<sup>-/-</sup>  
347 mice were done at the University of Liverpool with the approval of the UK Home Office and  
348 the University of Liverpool ethics committee. MRC-1<sup>-/-</sup> mice<sup>29</sup> were generated on a mixed  
349 129SvJ and C57BL/6 background, and then backcrossed to C57BL/6 strain for at least 7  
350 generations. Homozygous knockout mice were bred and maintained at the University of  
351 Nottingham and were a generous gift of Dr. Luisa Martinez-Pomares (University of  
352 Nottingham). WT and MRC-1<sup>-/-</sup> mice used for infection were sex and age matched and no more  
353 than 12 weeks of age at the start of the experiment. WT and MRC-1<sup>-/-</sup> mice were randomised

354 independently to time points by technical staff with no role in study design. Researchers were  
355 blinded to the experimental group until the data analysis stage. For experiments with MRC<sup>-/-</sup>  
356 mice, sample size calculations were not performed due to limited mice availability from our  
357 collaborators.

### 358 **Pneumococcal nasopharyngeal carriage model**

359 For induction of pneumococcal nasopharyngeal carriage, mice were lightly anaesthetized and  
360 10 µl PBS containing 1x10<sup>5</sup> CFU D39 was administered into the nostrils. The dose was  
361 confirmed by viable count following infection. At pre-chosen time intervals following  
362 infection, mice were sacrificed and nasopharynx, draining cervical lymph nodes and lungs were  
363 collected, passed through a 30 µm cell strainer or homogenized with an Ultra-Turrax T8  
364 homogeniser (IKA, Germany). Bacterial counts were determined from tissue homogenates by  
365 viable count on blood agar plates.

### 366 **Invasive pneumococcal disease model**

367 Mice were sedated by inhalation of 4% isoflurane and 50 µl PBS containing 10<sup>6</sup> CFU of wild-  
368 type T4 or the PLY mutant, T4Δply was administered into the nostrils. To block MRC-1, 20 µl  
369 of 0.1 mg/mL monoclonal anti-MRC-1 (Abcam) or isotype matched control (Abcam) was  
370 administered intranasally 30 min before infection. Post sacrifice, the lungs were perfused twice  
371 with ice-cold PBS containing 1 mM EDTA to collect the bronchoalveolar lavage fluid (BALF).  
372 To determine viable bacterial counts, serial dilutions of BALF were plated on blood agar plates  
373 followed by colony counting. Aliquots of BALF were frozen at -80°C for cytokine  
374 quantification by ELISA. To isolate alveolar macrophages, BALF was spun down at 400 g for  
375 7 min at 4°C, resuspended in R10 medium (RPMI 1640 containing 2 mM L-glutamine and 10%  
376 foetal bovine serum (FBS)) and plated on coverslips for 1 hr to allow cells to attach. Unattached  
377 cells were removed by washes with PBS. Macrophages were verified phenotypically by flow

378 cytometry (CD11c<sup>+</sup> Siglec F<sup>+</sup>). The percentage of neutrophils (CD11b<sup>hi</sup> Ly6G<sup>hi</sup>) and monocytes  
379 (CD11b<sup>hi</sup> Ly6C<sup>hi</sup>) in the BALF was quantified by flow cytometry upon gating for viable cells  
380 stained using fixable viable dye eFluor 780 (Thermo Fisher Scientific).

### 381 **MRC-1 knockdown using siRNA**

382 DCs (6 x 10<sup>6</sup>) were electroporated with 5 μM siRNA from Life Technologies against MRC-1  
383 (s53926, s53927, s53928) or scrambled control siRNA (4390843, 4390846) on day 4 of DC  
384 differentiation. The cells were electroporated with the Bio-Rad gene pulser (square wave, 500V,  
385 0.5 ms with a single impulse) and immediately resuspended in fresh R10 medium. The cells  
386 were used 48 hrs post siRNA electroporation. Treatment with siRNA reduced MRC-1 protein  
387 expression by ~80% as evaluated by western blotting (Fig. S3A).

### 388 **Flow Cytometry**

389 Cells were fixed with 4 % PFA and stained with a mouse anti-MRC-1 (Abcam) and a goat-anti  
390 mouse Alexa Fluor 488 secondary antibody (Life Technologies). For intracellular staining, cells  
391 were fixed with 4% PFA and permeabilized with ice cold methanol. Cells were stained with  
392 phospho-STAT1 (Tyr 701) Alexa Fluor 488 conjugated rabbit antibody (Cell Signalling), rabbit  
393 anti-SOCS1 (ab135718) and assessed by flow cytometry using the Gallios Flow Cytometer. In  
394 addition, the following antibodies from Biolegend were used in this study : CD3 (100235), CD4  
395 (100405), CD8a (100707), CD11b (101207), CD19 (152403), CD45 (103111), CD69 (104507),  
396 CD115 (135523), CD206 (MRC-1) (141707), F4/80 (123107), FOXP3 (126403), GATA3  
397 (653805), Gr-1 (108411), MARCO (BioRad ED31), RORγt (654301), T-bet (644809).  
398 Antibodies were conjugated to fluorescein isothiocyanate (FITC), phycoerythrin (PE), PE-Cy7  
399 or allophycocyanin (APC) and appropriate isotype controls were included in all experiments.

### 400 **Quantification of cytokines**

401 For cytokine measurement, cell-free culture supernatants were harvested 18 hrs pi and frozen  
402 at -20°C. The levels of human TNF-α, IL-12p70, IL-1β, IFN-γ and IL-4, using the OptEIA™

403 ELISA kit (BD Biosciences). The levels of mouse TNF- $\alpha$ , IL-12p70, IL-1 $\beta$ , IL-10 and TGF- $\beta$   
404 in the mouse BALF was measured using the respective mouse ELISA kits (BD Biosciences).

#### 405 **Enzymatic deglycosylation of PLY**

406 PLY was deglycosylated under native conditions using the Protein Deglycosylation kit (Sigma)  
407 following the instructions of the kit. Briefly, 10  $\mu$ g of recombinant PLY was incubated with 1  
408  $\mu$ l each of Peptide:N-glycosidase F, O-Glycosidase, Sialidase A,  $\beta$ -(1-4)-Galactosidase and  $\beta$ -  
409 N-acetylglucosaminidase in 50  $\mu$ l reaction buffer for 3 days at 37°C. The extent of  
410 deglycosylation was assessed by mobility shifts on SDS-PAGE gels.

#### 411 **Pull-down of PLY-interacting proteins and Co-IP with MRC-1**

412 To identify proteins interacting with PLY, pull-down was performed on DC and THP-1 native  
413 cell lysates using recombinant PLY as the bait. Cells were lysed with native lysis buffer  
414 (Abcam) containing 1x protease inhibitors (Roche) on ice for 15 min. Briefly, lysate  
415 corresponding to 0.8 mg protein was precleared by incubating with Protein G-agarose beads  
416 (Pierce) for 30 min at 4°C. Subsequently, the precleared lysate was incubated with 1  $\mu$ g PLY  
417 (Cusabio) for 1 hr at 4°C and then incubated with Protein G beads conjugated to mouse anti-  
418 PLY (Abcam) with gentle rotation overnight at 4°C. As a control, lysates were incubated with  
419 isotype antibody or beads alone to distinguish non-specific interactions. The beads were washed  
420 thrice with PBS and the bound proteins were eluted by boiling in NuPAGE LDS sample buffer  
421 for 5 min at 95°C. The eluted proteins were identified using mass spectrometry at the Science  
422 for Life Laboratory in Uppsala, Sweden. The protein identifications were based on at least two  
423 matching peptides of 95% confidence per protein. To confirm the interaction between PLY and  
424 MRC-1, western blotting was performed on the eluate. MRC-1 was detected using rabbit anti-  
425 human MRC-1 (Abcam) and HRP-conjugated secondary goat anti-rabbit (GE Healthcare).

426

## 427 **Surface plasmon resonance analysis**

428 Surface plasmon resonance experiments were run on Biacore 3000 and T200 instruments (GE  
429 Healthcare) at 25°C with 10 mM HEPES Supplementaryemented with 2 mM CaCl<sub>2</sub> and 0.1 %  
430 (v/v) Tween 20 as running buffer. Pneumolysin (PLY; Causabio) and mannose receptor C type  
431 1 (MRC-1; R&D Systems) were diluted to 10 µg/mL in 10 mM NaOAc pH 4.5 and immobilized  
432 on CM5 chips by amine coupling to immobilization levels of 2200 and 12000 RU, respectively.  
433 PLY was buffer-exchanged into running buffer using a 3 kDa MWCO Amicon centrifugal filter  
434 device prior to injections. Human serum albumin was immobilized at 11000 RU in a separate  
435 flow cell as a negative control. Analytes were injected at 30 µl/min and surfaces were  
436 regenerated using 10 mM HCl. Sensorgrams were double referenced using a blank flow cell  
437 and a buffer injection. Data for injections of PLY over MRC-1 were fitted to a Langmuir 1:1  
438 interaction using BiaEval 4.1 software and the dissociation equilibrium constant was calculated  
439 from average association and dissociation rate constants obtained from three separate dilution  
440 series analyzed on two different sensor chips. Human serum albumin, bovine serum albumin  
441 and Trastuzumab (Herceptin®) were injected at 1 µM as negative controls for non-specific  
442 binding. The influence of mannose on MRC-1 binding was evaluated by pre-incubating 100  
443 nM of MRC with 0.5 mM D-mannose or D-glucose (Sigma) for 1 hr in running buffer prior to  
444 injection of the mixed samples over the PLY immobilized chip.

## 445 **ELISA to measure MRC-1-PLY binding**

446 Briefly, 96-well flat-bottomed plates (Sigma, UK) were coated overnight with 1.25-10 µg/ml  
447 of mannose receptor, full-length (2534-MR-050) or truncated constructs CTLD4-7-Fc, CR-  
448 FNII-CTLD1-3-Fc<sup>30</sup>, a generous gift from Dr Luisa Martinez-Pomares (University of  
449 Nottingham, UK), in the presence or absence of galactose or mannose (Sigma, UK) in coating  
450 buffer (15 mM Na<sub>2</sub>CO<sub>3</sub>, 35 mM NaHCO<sub>3</sub>, pH 9.6). Wells were blocked with 200 µl of 20%  
451 (v/v) FBS in PBS for 2 hrs, and then washed three times with 250 µl PBS, 0.05% (v/v) Tween

452 20 (Sigma, UK). 10 µg/ml of PLY, PdB, PLY domains 1-3 or PLY domain 4 was added and  
453 incubated at 37°C for 1 hr. Wells were washed again with PBS and bound proteins were detected  
454 using PLY polyclonal antibody (Abcam ab71811) in blocking buffer. Plates were incubated  
455 with anti-rabbit IgG alkaline phosphatase (Abcam ab6722) in blocking buffer. Bound  
456 antibodies were detected in using the chromogenic substrate p-nitrophenylphosphate (pNPP)  
457 for 30 min. 1M NaOH was added to all wells and the absorbance was measured at 405 nm.

458 To study the specific interaction of MRC-1 with PLY versus capsular polysaccharides,  
459 immobilized MRC1 was incubated with PLY (0-5 µg/ml) in the presence or absence of 2.5  
460 µg/ml of purified serotype 2 or type 4 capsules (SSI Diagnostica). Bound PLY in the presence  
461 or absence of capsule was detected using mouse anti-PLY and anti-mouse IgG-HRP. Binding  
462 of purified capsule to MRC-1 was detected using rabbit anti-capsule and anti-rabbit IgG-HRP.  
463 Bound antibodies were detected using the chromogenic substrate, tetramethylbenzidine (TMB).  
464 1M phosphoric acid was used as stop solution and absorbance was measured at 450 nm.

#### 465 **Immunofluorescence microscopy**

466 Briefly, cells were fixed with 4% paraformaldehyde buffered in PBS for 10 min. Subsequently,  
467 the cells were permeabilized using PBS containing 0.5% Tween20 for 15 min. To block non-  
468 specific interactions, cells were incubated with 5% FBS in PBS for 1 hr. Lysosomes were  
469 stained using lysotracker deep red (Thermo Fisher Scientific) prior to fixation. Early endosomes  
470 were stained using Alexa 647conjugated anti-EEA1 (Abcam). PLY was stained using mouse  
471 anti-PLY (Abcam) and Alexa488-goat anti-mouse secondary antibody (Thermo Fisher  
472 Scientific). MRC-1 was detected using rabbit anti-MRC-1 (Abcam) and Alexa 555-goat anti-  
473 rabbit secondary antibody (Thermo Fisher Scientific). Pneumococci were stained using rabbit  
474 anti-pneumococcal anti-serum (Eurogentec) labeled with Alexa 488 using Zenon rabbit IgG  
475 labeling kit (Thermo Fisher Scientific). Type 1 clinical strains were stained using anti-serum  
476 Type 1 (Statens Serum Institut). Samples were washed twice with PBS between the antibody

477 incubations and mounted on slides using ProLong Diamond antifade reagent containing DAPI  
478 (Thermo Fisher Scientific). Images were acquired using the Delta Vision Elite microscope  
479 under the 100x objective (GE Healthcare).

#### 480 **Immunohistochemistry**

481 Draining cervical lymph nodes were snap frozen in liquid nitrogen and 7  $\mu\text{m}$  sections were cut.  
482 Staining was performed with fluorochrome conjugated MRC-1 (biotin 647, BD biosciences)  
483 and appropriate isotype matched controls. Sections were mounted in ProLong Gold  
484 (Invitrogen) and images were taken using a Zeiss Axioplan LSM 510 confocal microscope as  
485 single optical slices of between 0.8 and 1.0  $\mu\text{m}$ . Images were analyzed using Zeiss LSM image  
486 browsing software v4.

#### 487 **Western blotting**

488 Cells were lysed with RIPA buffer containing 1 $\times$  protease inhibitors (Roche) on ice for 15  
489 minutes. Cell debris and nuclear material were pelleted by centrifuging at 13000 rpm for 15  
490 min. Lysate corresponding to 25  $\mu\text{g}$  protein was boiled for 5 min at 95 $^{\circ}\text{C}$  in NuPAGE LDS  
491 sample buffer and resolved on 4-12% Bis-Tris gel (Invitrogen). Proteins were transferred to  
492 polyvinylidene fluoride (PDVF) membrane and blocked with 5% skim milk powder in PBS  
493 containing 0.1% Tween-20. Proteins were detected using the following antibodies: mouse anti-  
494 human MRC-1 (Abcam), SOCS1 antibody, NF $\kappa$ B(p65) antibody (Santa Cruz) and a phospho-  
495 I $\kappa$ Ba (Ser32) (Santa Cruz). Rabbit anti-GAPDH (Sigma) and Rabbit Histone H2A2.Z (Cell  
496 signaling Technologies) was used as a loading control. Anti-rabbit IgG or anti-mouse IgG  
497 conjugated to horseradish peroxidase (GE Healthcare) were used as secondary antibodies. Blots  
498 were developed with Amersham<sup>TM</sup> ECL Plus Western blotting detection system (GE  
499 Healthcare), using a ChemiDoc<sup>TM</sup> XRS+ (Bio-Rad Laboratories).

#### 500 **Statistical analysis**

501 Data were statistically analysed using GraphPad Prism 5.04. Data of immune cells prepared  
502 from human donor blood were analysed with a Wilcoxon matched-pairs signed rank test. Data  
503 from THP-1 macrophages were analysed with a Mann Whitney test. Comparison between  
504 groups was done with a one-way or two-way ANOVA followed by a Bonferroni or Tukey's  
505 post-test as indicated. Normalized data was analysed with an unpaired t-test. Differences were  
506 considered significant at \*P < 0.05, \*\*P < 0.005 and ns denotes not significant.

### 507 **Life Sciences Reporting Summary**

508 Further information on experimental design is available in the Life Sciences Reporting  
509 Summary.

### 510 **Data availability**

511 The data that support the findings of this study are available from the corresponding authors  
512 upon reasonable request.

513

514 **References**

- 515 1 Black, R. E. *et al.* Global, regional, and national causes of child mortality in 2008: a systematic  
516 analysis. *Lancet* **375**, 1969-1987, doi:10.1016/S0140-6736(10)60549-1 (2010).
- 517 2 Berry, A. M., Yother, J., Briles, D. E., Hansman, D. & Paton, J. C. Reduced virulence of a defined  
518 pneumolysin-negative mutant of *Streptococcus pneumoniae*. *Infection and immunity* **57**,  
519 2037-2042 (1989).
- 520 3 Hirst, R. A. *et al.* *Streptococcus pneumoniae* deficient in pneumolysin or autolysin has reduced  
521 virulence in meningitis. *The Journal of infectious diseases* **197**, 744-751, doi:10.1086/527322  
522 (2008).
- 523 4 Zafar, M. A., Wang, Y., Hamaguchi, S. & Weiser, J. N. Host-to-Host Transmission of  
524 *Streptococcus pneumoniae* Is Driven by Its Inflammatory Toxin, Pneumolysin. *Cell Host*  
525 *Microbe* **21**, 73-83, doi:10.1016/j.chom.2016.12.005 (2017).
- 526 5 Paton, J. C., Rowan-Kelly, B. & Ferrante, A. Activation of human complement by the  
527 pneumococcal toxin pneumolysin. *Infection and immunity* **43**, 1085-1087 (1984).
- 528 6 Iliev, A. I., Djannatian, J. R., Nau, R., Mitchell, T. J. & Wouters, F. S. Cholesterol-dependent actin  
529 remodeling via RhoA and Rac1 activation by the *Streptococcus pneumoniae* toxin  
530 pneumolysin. *Proceedings of the National Academy of Sciences of the United States of America*  
531 **104**, 2897-2902, doi:10.1073/pnas.0608213104 (2007).
- 532 7 McNeela, E. A. *et al.* Pneumolysin activates the NLRP3 inflammasome and promotes  
533 proinflammatory cytokines independently of TLR4. *PLoS Pathog* **6**, e1001191,  
534 doi:10.1371/journal.ppat.1001191 (2010).
- 535 8 Price, K. E. & Camilli, A. Pneumolysin localizes to the cell wall of *Streptococcus pneumoniae*. *J*  
536 *Bacteriol* **191**, 2163-2168, doi:10.1128/JB.01489-08 (2009).
- 537 9 Gordon, S. Alternative activation of macrophages. *Nature reviews. Immunology* **3**, 23-35,  
538 doi:10.1038/nri978 (2003).
- 539 10 Kang, P. B. *et al.* The human macrophage mannose receptor directs *Mycobacterium*  
540 *tuberculosis* lipoarabinomannan-mediated phagosome biogenesis. *J Exp Med* **202**, 987-999,  
541 doi:10.1084/jem.20051239 (2005).
- 542 11 Taylor, P. R., Gordon, S. & Martinez-Pomares, L. The mannose receptor: linking homeostasis  
543 and immunity through sugar recognition. *Trends in immunology* **26**, 104-110,  
544 doi:10.1016/j.it.2004.12.001 (2005).
- 545 12 Zamze, S. *et al.* Recognition of bacterial capsular polysaccharides and lipopolysaccharides by  
546 the macrophage mannose receptor. *The Journal of biological chemistry* **277**, 41613-41623,  
547 doi:10.1074/jbc.M207057200 (2002).
- 548 13 McGreal, E. P. *et al.* The carbohydrate-recognition domain of Dectin-2 is a C-type lectin with  
549 specificity for high mannose. *Glycobiology* **16**, 422-430, doi:10.1093/glycob/cwj077 (2006).
- 550 14 Macedo-Ramos, H. *et al.* Evidence of involvement of the mannose receptor in the  
551 internalization of *Streptococcus pneumoniae* by Schwann cells. *BMC Microbiol* **14**, 211,  
552 doi:10.1186/s12866-014-0211-9 (2014).
- 553 15 Macedo-Ramos, H. *et al.* Olfactory ensheathing cells as putative host cells for *Streptococcus*  
554 *pneumoniae*: evidence of bacterial invasion via mannose receptor-mediated endocytosis.  
555 *Neurosci Res* **69**, 308-313, doi:10.1016/j.neures.2010.12.015 (2011).
- 556 16 Kadioglu, A., Weiser, J. N., Paton, J. C. & Andrew, P. W. The role of *Streptococcus pneumoniae*  
557 virulence factors in host respiratory colonization and disease. *Nat Rev Microbiol* **6**, 288-301,  
558 doi:10.1038/nrmicro1871 (2008).
- 559 17 Yoshimura, A., Naka, T. & Kubo, M. SOCS proteins, cytokine signalling and immune regulation.  
560 *Nat Rev Immunol* **7**, 454-465, doi:10.1038/nri2093 (2007).
- 561 18 Yasukawa, H., Sasaki, A. & Yoshimura, A. Negative regulation of cytokine signaling pathways.  
562 *Annu Rev Immunol* **18**, 143-164, doi:10.1146/annurev.immunol.18.1.143 (2000).

- 563 19 Chieppa, M. *et al.* Cross-linking of the mannose receptor on monocyte-derived dendritic cells  
564 activates an anti-inflammatory immunosuppressive program. *J Immunol* **171**, 4552-4560  
565 (2003).
- 566 20 Paton, J. C. *et al.* Purification and immunogenicity of genetically obtained pneumolysin toxoids  
567 and their conjugation to *Streptococcus pneumoniae* type 19F polysaccharide. *Infect Immun*  
568 **59**, 2297-2304 (1991).
- 569 21 Guilliams, M., Bruhns, P., Saeys, Y., Hammad, H. & Lambrecht, B. N. The function of Fcγ  
570 receptors in dendritic cells and macrophages. *Nat Rev Immunol* **14**, 94-108,  
571 doi:10.1038/nri3582 (2014).
- 572 22 Littmann, M. *et al.* *Streptococcus pneumoniae* evades human dendritic cell surveillance by  
573 pneumolysin expression. *EMBO Mol Med* **1**, 211-222, doi:10.1002/emmm.200900025 (2009).
- 574 23 Rajaram, M. V. S. *et al.* M. tuberculosis-Initiated Human Mannose Receptor Signaling Regulates  
575 Macrophage Recognition and Vesicle Trafficking by Fcγ-Chain, Grb2, and SHP-1. *Cell*  
576 *Rep* **21**, 126-140, doi:10.1016/j.celrep.2017.09.034 (2017).
- 577 24 Sakaguchi, S., Miyara, M., Costantino, C. M. & Hafler, D. A. FOXP3+ regulatory T cells in the  
578 human immune system. *Nat Rev Immunol* **10**, 490-500, doi:10.1038/nri2785 (2010).
- 579 25 Schuette, V. *et al.* Mannose receptor induces T-cell tolerance via inhibition of CD45 and up-  
580 regulation of CTLA-4. *Proc Natl Acad Sci U S A* **113**, 10649-10654,  
581 doi:10.1073/pnas.1605885113 (2016).
- 582 26 Neill, D. R. *et al.* Density and duration of pneumococcal carriage is maintained by transforming  
583 growth factor beta1 and T regulatory cells. *Am J Respir Crit Care Med* **189**, 1250-1259,  
584 doi:10.1164/rccm.201401-0128OC (2014).
- 585 27 Dorrington, M. G. *et al.* MARCO is required for TLR2- and Nod2-mediated responses to  
586 *Streptococcus pneumoniae* and clearance of pneumococcal colonization in the murine  
587 nasopharynx. *J Immunol* **190**, 250-258, doi:10.4049/jimmunol.1202113 (2013).
- 588 28 Shak, J. R. *et al.* Novel role for the *Streptococcus pneumoniae* toxin pneumolysin in the  
589 assembly of biofilms. *mBio* **4**, e00655-00613, doi:10.1128/mBio.00655-13 (2013).
- 590 29 McKenzie, E. J. *et al.* Mannose receptor expression and function define a new population of  
591 murine dendritic cells. *J Immunol* **178**, 4975-4983 (2007).
- 592 30 Martinez-Pomares, L. *et al.* Carbohydrate-independent recognition of collagens by the  
593 macrophage mannose receptor. *European journal of immunology* **36**, 1074-1082,  
594 doi:10.1002/eji.200535685 (2006).

595

596

597

598

599

600

601 **Correspondence** should be addressed to Prof. Birgitta Henriques-Normark  
602 (birgitta.henriques@ki.se) and Prof. Aras Kadioglu (a.kadioglu@liverpool.ac.uk)

### 603 **Acknowledgments**

604 The work in Sweden was supported by grants from the Swedish Research Council, Stockholm  
605 County Council, the Swedish Foundation for Strategic Research (SSF), and the Knut and Alice  
606 Wallenberg foundation. The work in Liverpool was supported by funding from the UK Medical  
607 Research Council (Programme Grant Number MR/P011284/1), a Sir Henry Dale Fellowship  
608 (awarded to D.R.N.) and jointly funded by the Wellcome Trust and the Royal Society (Grant  
609 Number 204457/Z/16/Z), a British Commonwealth Scholarship (awarded to S.K.), Embassy of  
610 the Kingdom of Saudi Arabia Scholarship (awarded to H.M.) and the Institute of Infection &  
611 Global Health, University of Liverpool. We thank the Science for Life Laboratory Mass  
612 Spectrometry Based Proteomics Facility in Uppsala for the LC-MS analysis.

### 613 **Author contributions**

614 K.S, D.R.N, L.S, A.K and B.H.N designed the study. K.S., L.S., G.D.M, H.M., S.K, E.D, M.Y,  
615 A.K, D.R.N, A.A., J.N., P.N and L.P performed experiments. K.S, L.S, D.R.N., A.K and BHN  
616 wrote the manuscript, and the other authors contributed to writing. All authors read and  
617 approved the final version of the manuscript.

### 618 **Competing interests**

619 The authors declare that no competing interests exist.

620

621

622 **Figure legends**

623 **Fig. 1. Pneumolysin inhibits cytokine responses and inflammatory signalling in DCs by**  
624 **upregulating SOCS1. (a)** TNF- $\alpha$  secretion from human dendritic cells (DCs) (N=6), THP-1  
625 macrophages (N=4), and primary neutrophils (N=4) upon infection with wild type strain T4R  
626 or its isogenic pneumolysin (PLY) mutant T4R $\Delta$ *ply*. Data are mean $\pm$ SEM. \*P < 0.05 by  
627 Wilcoxon matched-pairs signed (two-tailed) rank test. **(b)** TNF- $\alpha$  secretion from DCs infected  
628 with encapsulated strains, T4 or T4 $\Delta$ *ply* (N=3 donors). Data are mean $\pm$ S.E.M. P < 0.05 by  
629 Wilcoxon matched-pairs signed (two-tailed) rank test. **(c)** SOCS1 mRNA levels in T4R or  
630 T4R $\Delta$ *ply* infected DCs at 9 hrs post infection (pi) (N=3 donors). Data are mean $\pm$ S.E.M. P <  
631 0.05 by paired two-tailed t test. **(d)** Flow cytometry histogram plot showing SOCS1 protein  
632 levels in T4R or in T4R $\Delta$ *ply* infected DCs at 9 hrs pi. Percentage of SOCS1<sup>+</sup> cells is indicated  
633 within the parenthesis. **(e)** STAT1 phosphorylation in T4R or in T4R $\Delta$ *ply* infected DCs at 3-5  
634 hrs pi. Data in d,e are representative of 3 independent experiments. **(f)** Western blot showing  
635 the levels of nuclear NF- $\kappa$ B (p65) in T4R or T4R $\Delta$ *ply* infected DCs at 4 hrs pi. Histone H2A  
636 served as loading controls. Blots are representative of data from 2 independent experiments.

637 **Fig. 2. MRC-1 co-localizes with pneumolysin and intracellular pneumococci in DCs. (a)**  
638 Representative sensorgram of three independent surface plasmon resonance experiments  
639 showing the dose-dependent binding profile of recombinant PLY (12.5-200 nM) over  
640 immobilized MRC-1. **(b)** ELISA showing the binding of immobilized MRC-1 constructs,  
641 CTLD4-7-Fc or CR-FNII-CTLD1-Fc (1.25-10  $\mu$ g/ml) with full-length pneumolysin (PLY),  
642 toxoid PdB, PLY domains 1-3 and domain 4. Mannan (Man) was used as a specific ligand for  
643 CTLD4-7 to block interaction with PLY, and galactose (Gal) was used as a negative control for  
644 the blocking assay. Bound PLY was detected using anti-PLY antibodies. Data are mean $\pm$ S.E.M  
645 of two independent experiments, each containing 3 replicates per condition. **(c)** Wild type (WT)

646 DCs or MRC-1 siRNA treated DCs were incubated with purified active PLY or mutant PLY  
647 (PdB) (200 ng/ml) for 45 min. Immunofluorescence staining show that active PLY co-localizes  
648 with MRC-1 and EEA-1 (early endosomes) in contrast to the non-pore forming mutant PLY  
649 (PdB). **(d)** DCs were infected with T4R or T4R $\Delta$ *ply* for 90 min. Immunofluorescence staining  
650 showed that intracellular T4R co-localizes with MRC-1, while T4R $\Delta$ *ply* does not co-localize  
651 with MRC-1, but with lysosomes (lysotracker) (white arrows). All scale bars, 5  $\mu$ m. Data in c,d  
652 are representative of three independent experiments.

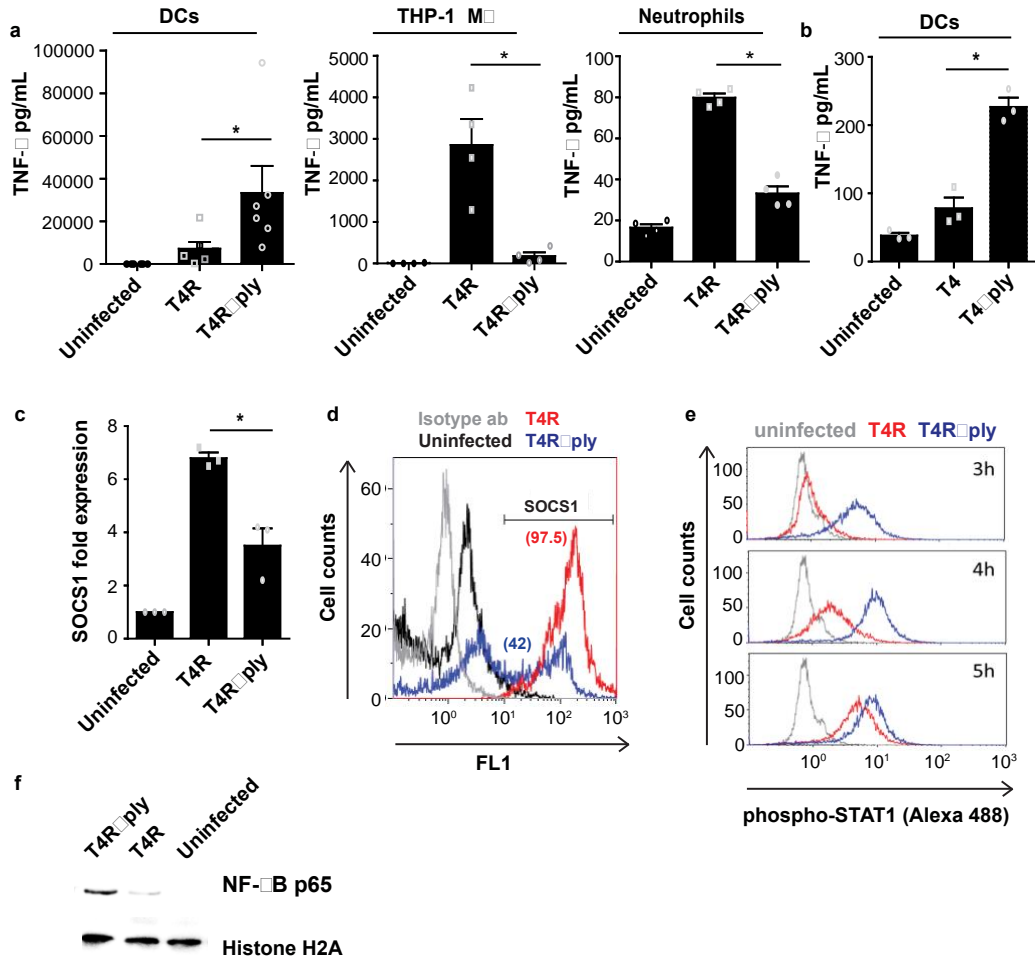
653 **Fig. 3. Depletion of MRC-1 abolishes pneumolysin induced cytokine inhibition and**  
654 **enhances T cell activation. (a)** Uptake of T4R and T4R $\Delta$ *ply* by WT and MRC-1 siRNA treated  
655 DCs (N=3 donors). The uptake was expressed as a percentage relative to untreated DCs. Data  
656 represent mean  $\pm$  S.E.M. \*\*\*\* denotes  $P < 0.0001$  by two-way ANOVA with Bonferroni post-  
657 test. **(b)** Wild type DCs (control) or MRC-1 siRNA treated DCs were infected with T4R and  
658 secretion of IL-12, TNF- $\alpha$  and IL-6 was measured in culture supernatants (N=3 donors). Data  
659 represent mean  $\pm$  S.E.M. \*\*\*\* denotes  $P < 0.0001$  and \*\* denotes  $P < 0.01$  by two-way ANOVA  
660 with Bonferroni post-test. **(c-d)** Wild type or MRC-1 siRNA treated DCs were infected with  
661 T4R, T4R $\Delta$ *ply* or recombinant PLY (rPLY) (200 ng/mL) for 24 hrs and co-cultured with naïve  
662 CD4<sup>+</sup> T cells for 5 days. Secretion of **(c)** IFN- $\gamma$  and **(d)** IL-4 was measured in culture  
663 supernatants (N=5 donors). Data represent mean  $\pm$  S.E.M. \*\*\*\* denotes  $P < 0.0001$ , \*\* denotes  
664  $P < 0.01$ , \* denotes  $P < 0.05$  by two-way ANOVA with Bonferroni post-test. **(e)** FoxP3 expression  
665 in human naïve CD4<sup>+</sup> T cells upon co-culture with DCs (control or MRC-1 siRNA treated)  
666 infected with T4R or T4R $\Delta$ *ply*. Data are representative of three independent experiments. **(f)**  
667 Percentage FoxP3<sup>+</sup> CD4<sup>+</sup> T cells upon co-culture with murine BMDMs (from wild type or  
668 MRC-1<sup>-/-</sup> mice) that were infected with heat-killed strain D39 or mutant derivatives lacking  
669 capsule (D39 $\Delta$ *cps*), PLY (D39 $\Delta$ *ply*) or a double mutant (D39 $\Delta$ *cps* $\Delta$ *ply*) or purified PLY. Data

670 represent mean  $\pm$  S.E.M. N=3, two way-ANOVA with Bonferroni multiple comparison test. \*  
671  $P < 0.05$ ; \*\* $P < 0.01$ .

672 **Fig. 4. MRC-1 mediates pneumolysin-induced suppression of early inflammatory**  
673 **responses *in vivo*.** (a) Primary alveolar macrophages were isolated from C57/BL6J mice  
674 infected with T4 or T4 $\Delta$ ply at 6 hrs pi. Immunofluorescence staining showed that PLY  
675 proficient pneumococci (T4) co-localize with MRC-1 unlike T4 $\Delta$ ply that co-localizes with the  
676 lysosome marker (lysotracker). Scale bars, 5 $\mu$ m. Images are representative of data from 5  
677 mice/group. (b) TNF- $\alpha$  levels (N=12) and (c) bacterial count (CFU/mL) (N=13) in BALF from  
678 mice infected with either T4 or T4 $\Delta$ ply at 6 hrs pi. Data are mean  $\pm$  S.E.M of three independent  
679 experiments. \*\* $P < 0.01$  by Mann-Whitney (two-tailed) test. (d) Levels of TNF- $\alpha$  (N=8), and  
680 (e) bacterial count (CFU/mL) (N=9) in BALF of mice pretreated with anti-MRC-1 (0.1 mg/mL)  
681 or isotype antibody and infected with strain T4 for 6 hrs. Data are mean  $\pm$  S.E.M of three  
682 independent experiments. \*\* $P < 0.01$  by Mann-Whitney (two-tailed) test. (f) Bacterial count  
683 (CFU) per mg nasopharyngeal homogenates of wild type or MRC-1<sup>-/-</sup> mice infected with strain  
684 D39 over a 14 day carriage experiment. N=6 per data point, data represent mean  $\pm$  S.E.M. and  
685 analyzed by two-way ANOVA with Tukey's post-test. (g) Model suggested for PLY-mediated  
686 immunomodulation. PLY-proficient pneumococci induce internalization into alveolar  
687 macrophages and DCs via interaction with MRC-1. PLY-expressing pneumococci co-localize  
688 with MRC-1 in non-lysosomal compartments and block inflammatory cytokine secretion by  
689 upregulating SOCS1, thereby promoting regulatory T cell responses and bacterial survival in  
690 the airways. \*\* $P < 0.01$ , \*\*\*  $P < 0.001$ .

691

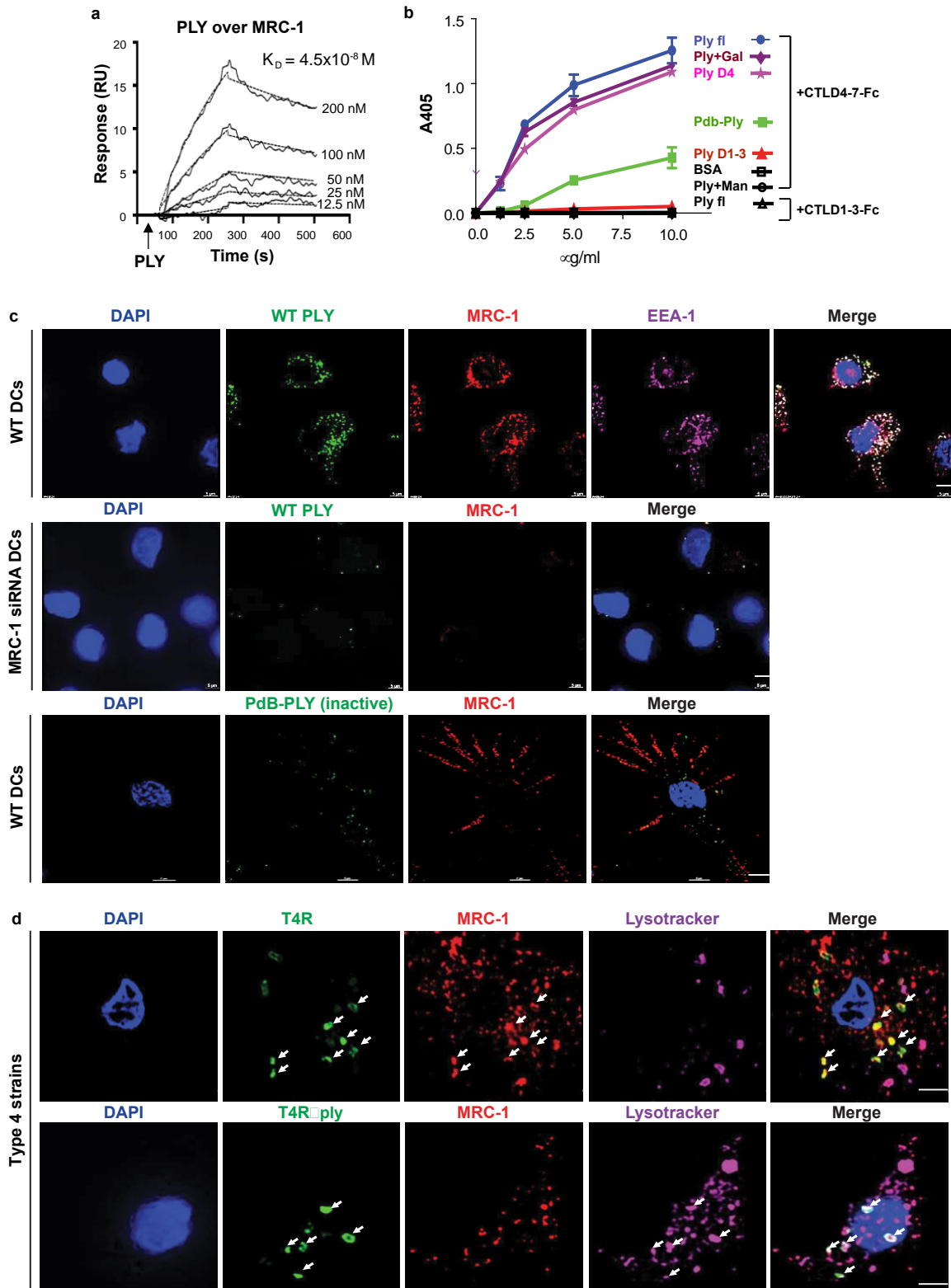
**Fig.1**



692

693

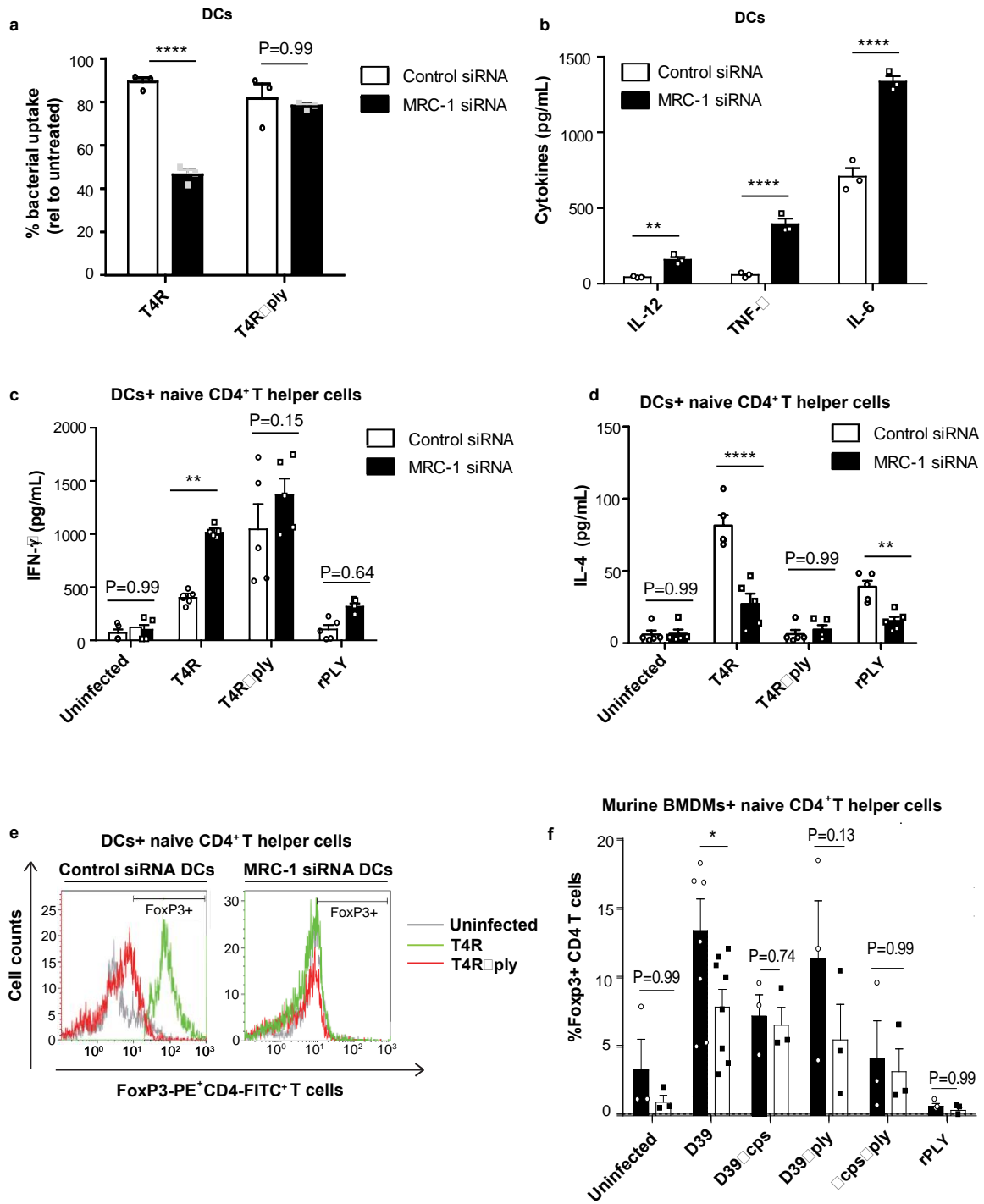
**Fig.2**



694

695

**Fig.3:**



696

697

**Fig.4**

